Available online at www.sciencedirect.com

ScienceDirect

Procedia Engineering 100 (2015) 105 – 114

Procedia Engineering

www.elsevier.com/locate/procedia

25th DAAAM International Symposium on Intelligent Manufacturing and Automation, DAAAM 2014

Analysis of Droplet Deposition in a Vertical Air-Water Dispersed Flow

Šikalo Šefko[a,*], Berberović Edin[b]

[a]*Faculty of Mechanical Engineering, University of Sarajevo, Vilsonovo Setaliste 9, 71000 Sarajevo, B&H*
[b]*Polytechnic Faculty, University of Zenica, Fakultetska 1, 72000 Zenica, B&H*

Abstract

Droplet deposition in a turbulent vertical air–water dispersed flow onto wall of a tube has been studied theoretically and experimentally. A model for the deposition of large droplets based on the droplet sticking efficiency to the tube wall is proposed. Sticking efficiency is defined as the ratio of the sticking mass flux to the impacting mass flux. The application of the proposed model is illustrated by calculating several quantities of a practical interest for analysis of heat and mass transfer in dispersed flows, namely the deposition coefficient onto dry wall, sticking efficiency onto wall liquid film and the minimum value of the liquid film Reynolds number at which a steady liquid film exist. The proposed model describes the change of the deposition coefficient with droplet concentration and fits the obtained deposition data satisfactorily for a wide range of the gas Reynolds numbers and droplet concentration. The model is useful for analysing of dryout and burnout heat transfer regimes.

Peer-review under responsibility of DAAAM International Vienna

Keywords: droplet deposition; dispersed flow; annular flow; deposition coefficient; droplet concentration

1. Introduction

Dispersed droplet flows occur in different types of industrial equipment, such as gas-liquid separators, gas-liquid mixers, evaporators, condensers, distillation columns, absorption and cooling towers. The dispersed droplet flow coexist either with a liquid film on the tube wall, as in the annular two-phase flow or in direct contact with the wall, as in the post-dryout regime.

* Corresponding author. Tel.: +387 33 729 892, fax: +387 33 653 055
E-mail address: sikalo@mef.unsa.ba

Peer-review under responsibility of DAAAM International Vienna
doi:10.1016/j.proeng.2015.01.348

Nomenclature

Latin symbols

c	Bulk droplet concentration, kg/m^3
D	Pipe diameter, m
d_{10}	Arithmetic mean diameter, m
d_{32}	Sauter mean diameter, m
F	Fraction deposition, -
k_D	Droplet deposition coefficient, m/s
k_D^+	Dimensionless deposition coefficient, -
l	Length in the flow direction, m
L	Length of the of pipe, m
M	Mass flow rate, kg/s
N_0	Flux of droplet deposition, kg/(m^{2}s)
p	Sticking efficiency, -
$\mathrm{Re_G}$	Gas-phase Reynolds number for a pipe, -
$\mathrm{Re_{LF}}$	Film Reynolds number, -
We	Weber number, -
$\mathrm{We_n}$	Normal Weber number, -
U	Gas velocity, m/s
u^*	Shear velocity, m/s

Greek symbols

α	Impact angle, °
μ	Viscosity, kg/(ms)
ρ	Density, kg/m^3
τ^+	The dimensionless inertial time constant of a droplet, -

Subscripts

G	gas phase
L	liquid
LE	entrained droplet
p	particle
in	inlet

The deposition process can be divided into two consecutive processes: the transport of particles to the wall and the adhesion of particles at the wall. The process of droplets deposition is known to be very complex.

For small droplet concentrations in gas core (c), the flux of droplet deposition (N_0) in vertical dispersed flow can be represented by the linear rate equation [1]

$$N_0 = k_D c \tag{1}$$

where k_D is the droplet deposition coefficient with units of velocity and c is the bulk concentration. The experimental data is usually presented as a dimensionless deposition coefficient $k_D^+ = k_D/u^*$ in terms of the dimensionless inertial time constant of a droplet τ^+, for a Stokes law resistance, where u^* is the friction (or shear) velocity in the pipe. The motion of a droplet in a turbulent flow mainly depends on the characteristic inertial time constant of the droplet, which characterizes the ability of a droplet to follow the fluid turbulence.

The available theoretical and experimental studies on the deposition of particles are reviewed in [2,3]. In these studies the research is divided into horizontal and vertical flows and classified the experiments by the method by which droplets were produced and how the results were measured. Particles were either injected, or originated from the wall, or from a fully developed annular film. The total deposition coefficient was determined by turbulent dispersion and a near-wall deposition velocity. The latter was the sum of a non-diffusive term (due to the mean

convection of the flow and gravity) and a diffusive term. This diffusive term accounted for the diffusion-impaction deposition regime and the inertia-moderated deposition regime. The deposition flux is depending on the turbulent dispersion of the droplets. The dispersion depends on the turbulent kinetic energy of the gas.

The deposition rate with respect to particle inertia was represented with dimensionless deposition coefficient versus dimensionless inertial time constant of a droplet in [2,3]. According to these reviews of deposition data in vertical flow systems in the range of large droplets ($\tau^+ > 20$), a mean value of $k_D^+ = 0.18$ was found as a rough empirical fit of experimental results, although there is a significant scatter on experimental data. The maximum deposition coefficients are one order of magnitude larger than the minimum deposition coefficients, when these dimensionless quantities are employed. The size of the droplets in the annular flow is such that the dimensionless inertial time constant of the droplets is large, $\tau^+ > 20$.

For vertical flow systems, deposition data in the range of larger droplet diameter are reported in [4,5,6,7] for uniform-sized particles, and in [1,8,9,10,11,12,13] are involved droplet size distribution. The theoretical analysis of the deposition data of large droplets is reported in [14,15,16,17].

The droplet deposition coefficient k_D was first reported in [14] in terms of droplet concentration, where it was attributed to the effect of droplet concentration on the turbulence in the gas core. Empirical correlations for droplet deposition coefficient as a function of droplet concentration are proposed in [18,19,11]. However there is no general correlation based on the appropriate physical modelling.

The drop size distribution was measured in [20] and related to the deposition and the concentration in air-water flow. The arguments from [16] show that the deposition rate is proportional to the root-mean-square of the turbulent velocity fluctuations. It was also argued that the droplet deposition coefficient k_D varies as c^{-1}. From the consideration it is clear that a decrease in the deposition coefficient at larger droplet concentration cannot be explained solely by an increase in droplet size.

In [7] it was found that the presence of the water film on the wall impedes droplet deposition. It was suggested, as the most likely explanation, that the droplets bounced off the liquid film without adhesion with it.

The effect of the droplet sticking efficiency on the deposition rate was taken into account in [21]. Starting from fundamentals it was argued that droplet-droplet collisions are more likely to increase the time required for large droplets to reach the wall due to inelastic collisions diverting the droplets away from the walls. The model, which had empirical constants, had good agreement with both the high and the low liquid flow rate experiments.

Droplet deposition and entrainment in an upward annular flow was studied experimentally in [22]. Deposition mass transfer coefficients were shown to increase with increasing gas mass flux and decrease with increasing droplet concentration. Simple correlations were given for deposition at high and low droplet concentrations. High mass concentrations are those where droplet-droplet interactions become common which decreases the deposition coefficient. The deposition coefficients in [10] were shown to be larger at higher gas velocities and lower gas densities. An extensive review of various approaches to the calculation of droplet deposition coefficient has been given by Hanratty [23].

Most of the existing mathematical models are based on the assumption that droplets which reach the pipe wall or the film surface are deposited, or at least that a certain fraction of droplets deposit. Several authors have shown that the Weber number controls the probability of a droplet deposition on a liquid film. A relation between Weber number and deposition was demonstrated in [24,10,25].

The interaction of single droplets with different dry and wetted horizontal and inclined surfaces was experimentally and numerically studied in [26, 27]. The outcome of the impact depends on the droplet properties and the properties of the impacted surface. It was argued that the normal droplet impact Weber number (based on the normal component of the impact velocity) is an important dimensionless parameter to define the droplet impact outcomes. However, this number alone is not sufficient to classify different types of droplet impact. Different outcomes are observed, such as spread, spread and slide, slip and spread, splash in all directions, or only in the forward direction, rebound and partial rebound, depending on the impact angle, liquid and surface properties as well as the Reynolds and Weber numbers. The droplet impact outcomes are also reported in [28,29], where it was argued that the normal droplet impact Weber number is an important dimensionless parameter to define the droplet impact outcomes.

The computational and theoretical study of flows generated by drop collisions was performed in [30,31,32] comprising collision with a shallow liquid layer, binary drop collision, drop collision with a dry wall and drop impact onto a heated wall accounting for the heat transfer within the wall. In the case of the drop impact onto a liquid layer [30] a scaling relation for the residual liquid film thickness upon the impact was proposed based on the description of the film evolution and development of the viscous boundary layer. In binary drop collision and drop impact on a dry surface [31] the results have shown that if the impact Reynolds and Weber numbers are high enough, the flow in the liquid lamella formed upon the impact far from its edge is universal and the evolution of the lamella thickness almost does not depend on the viscosity and surface tension. In the nonisothermal drop impact configuration [32] the influence of the increasing impact velocity is, as expected, manifested through the increase in the amount of heat transferred from the hot substrate.

Measurements of the critical impact angle for a droplet to rebound (the limit droplet rebound/deposition) on a liquid film are presented in [28]. When the critical normal Weber number, $\mathrm{We}_{\mathrm{n,cr}} = \mathrm{We}\sin^2\alpha_{\mathrm{cr}}$, is plotted against the critical impact angle α_{cr} (measured from the wall plane), the data exhibit constant values of $\mathrm{We}_{\mathrm{n,cr}} = 5$. An angle of impact refers to the acute angle between the wall plane and the droplet velocity vector at the point of impact. Snapshots of an actual case of a rebound of a water droplet from the wall liquid film are shown in Fig. 1.

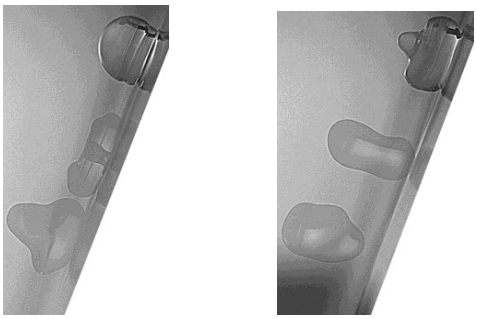

Fig. 1. Rebound of a water droplet from the wall liquid film (d_{p}=2.7 mm, α=22°, We_{n}=5.5).

For applications related to heat transfer in annular dispersed flows, the typical droplet impact angles are low (α<5°) and the normal Weber numbers ($\mathrm{We}_{\mathrm{n}} = \rho D u_n^2/\sigma$) based on the wall-normal velocity u_n ($u_{\mathrm{n}} = u\sin\alpha$) and the droplet diameter D are less than 5. For instance, The rate of deposition of 50 μm water droplets injected centrally into a downward flowing pipe flow at a gas Reynolds number of Re = 30600 was studied in [7]. The droplet impact angle was found to lie in the range 0.5°÷3.5° with a normal Weber number in the range $0.007<\mathrm{We}_{\mathrm{n}}<0.34$. A dispersed annular flow in vertical tubes at Re = 40000÷95000 was studied in [12], where impact angles of 0.5°÷1.5° were found. The droplet mean diameter ranged from 7 μm to 30 μm, yielding a normal Weber number in the range of $0.025<\mathrm{We}_{\mathrm{n}}<1.80$, similar to [7].

Due to its importance in engineering and industry, investigations relevant to droplet deposition in two-phase flows are continuously conducted and some of the more recent contributions are given in [33,34,35,36,37]

This paper presents experimental data and a model for relating deposition coefficient and droplet concentration in a turbulent flow. The experimental data obtained in an in-house laboratory for an adiabatic air–water system in a vertical stainless steel tube is analyzed. We assumed that all droplets impacting the dry surface stick to it, while a fraction of droplets impacting the liquid film rebounds. We could calculate the droplet sticking efficiency on the wall liquid film (the fraction of the droplets that merges to the liquid film) as the fitting parameter of experimental data. The length of tube covered with the smooth liquid film formed due to droplet deposition increases with increasing of the inlet droplet concentration.

2. Experimental apparatus

Experiments were carried out on a vertical upward air–water flow in a circular pipe of inner diameter 13.2 mm (stainless steel, SS 304, with average roughness R_a=3.37 μm). A schematic diagram of the loop is shown in Fig. 2. The setup includes a 792 mm long entrance section (60 tube diameters), in order to obtain a fully developed flow in the test section. The test section is 924 mm long (70 tube diameters). The water was supplied to the atomizer (7) from the water tank (4) by the gear pump (5). The flow rate was regulated by the pump rotation speed and a valve, and measured by a rotameter (6). After leaving the flow meter, water flows into the atomizer with a sharp-edged air orifice and the liquid nozzle generates the liquid droplets. The air from the compressor (1) passes first through the cyclone separator (2) and an oil filter to eliminate dust, moisture and oil contents, and then the air flows through the pressure tank and goes to the experimental section. The air flow rate was regulated by valves and measured by rotameters (3), with an accuracy of ±2%. The primary air flow (Q_p) is used to change the bulk flow rate in the test section, while the secondary air flow (Q_s) is used for the liquid atomization. An extraction unit (porous segments, 8) connected to the liquid separator (11) is used to remove the liquid wall film formed by the droplet deposition.

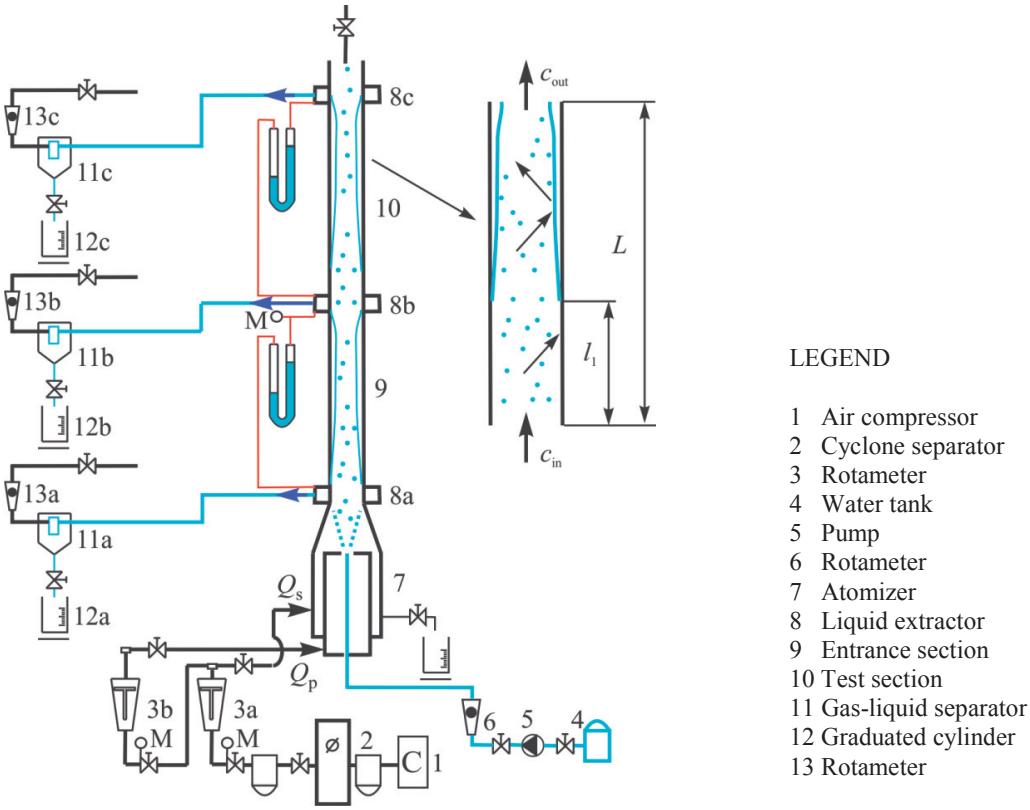

Fig. 2. Schematic diagram of the experimental apparatus.

The pressure in test section forced the liquid out of the pipe trough the extractor (8) into the cyclone gas–liquid separators (11) and water is collected into a measuring vessel (12). The gas take-off at the extractor (8) was typically around 0.5% of the total gas flow through the test section, and is considered to have no significant effect on the pressure drop. The liquid layer formed in the entrance section is completely removed. Observations of the deposition in a transparent pipe indicate that the droplets impinge on the wall forming larger droplets. They merge together forming rivulets which, at large flow rates, spread over the wall forming a continuous liquid film at a distance (l_1) from the inlet. The liquid film grows continuously along the test section (10). The liquid film is also being completely removed at the test section exit (extractor 8c). The flow rate of the liquid collected at the test section exit gives the average deposited rate over the test section length. The remaining liquid in the air–water droplet mixture past the top extractor is measured by removing the liquid in the cyclone separator. The liquid flow rates are measured by collecting the water in the measuring vessels (12) for a known period of time. This serves as a check on the overall mass balance. All the data is taken in a steady state condition.

3. Data analysis

The fractional deposition F in the test section is determined from the relation

$$F = \frac{M_{\mathrm{LE1}} - M_{\mathrm{LE2}}}{M_{\mathrm{LE1}}} \tag{2}$$

where M_{LE1} is the mass flow rate of the droplets in the gas flow at inlet of the test section and M_{LE2} is the mass flow rate of the droplets in the gas flow at the outlet of the test section. The deposition coefficient k_D is then calculated from a mass balance as

$$k_D = -\frac{U}{4}\frac{D}{L}\ln(1-F) \tag{3}$$

where U is the superficial gas velocity, D and L are the diameter and the length of the test section, respectively. The dimensionless deposition coefficient is given by $k_D^+ = k_D/u^*$, where u^*, the friction velocity is calculated from the measured pressure drop along the test section as $u^* = (\Delta pD/4\rho_{\mathrm{G}}L)^{1/2}$. The dimensionless inertial time constant of the droplet τ^+, based on the Stokes drag force, is calculated from the relation

$$\tau^+ = \frac{d_{10}^2 \rho_{\mathrm{G}} \rho_{\mathrm{p}} u^{*2}}{18\mu_{\mathrm{G}}^2} \tag{4}$$

where d_{10} is the arithmetic mean droplet diameter, calculated from the d_{32} using the relations developed in [38] as d_{10}=d_{32}/4.667. The Sauter mean diameter d_{32} is determined from the correlation given in [39], which is found to agree with the present drop size measurements.

The mass concentration of droplets in the gas core, at the inlet of the test section is calculated as

$$c_{\mathrm{in}} = \frac{M_{\mathrm{LE1}}}{M_{\mathrm{G}}/\rho_{\mathrm{G}}} \tag{5}$$

where M_{LE1} is the mass flow rate of droplets in the gas core, M_{G} is the mass flow rate of the gas and ρ_{G} is the gas density.

The aim of this study is to find a relation of the average droplet deposition coefficient in terms of the dimensionless droplet concentration, $k_D^+ = f(c_{\mathrm{in}}^+)$, taking into account the droplet sticking efficiency. The average droplet deposition coefficient k_D along the test section is determined experimentally. In this consideration, as proposed in [26], a part of the test section downstream of the inlet, of length l_1, can be assumed as the "dry" length, without droplet rebound. The remaining section length L–l_1 is the liquid film length, with sticking efficiency less than one. Therefore, the average droplet deposition coefficient is defined as

$$k_{\mathrm{D}} = k_{\mathrm{D1}} \frac{l_{\mathrm{l}}}{L} + k_{\mathrm{D2}} \frac{L - l_{\mathrm{l}}}{L} \tag{6}$$

where k_{D1} is the droplet deposition coefficient for the dry region of the test section and k_{D2} is the droplet deposition coefficient for the liquid film region. The relation for the average dimensionless droplet deposition coefficient in terms of the droplet dimensionless concentration is described in [12]:

$$k_D^+ = \begin{cases} k_{D1}^+, \text{ if } c_{\mathrm{in}}^+ \le c_{\mathrm{in,CR}}^+ \text{ or } (l_{\mathrm{l}} \ge L) \\ k_{D1}^+ p - (1-p)\frac{1}{4}\frac{U}{u^*}\frac{D}{L}\ln\left(1 - \frac{\mathrm{Re_{LFC}}}{\mathrm{Re}}\frac{\mu_L}{\mu_{\mathrm{G}}}\frac{1}{c_{\mathrm{in}}^+}\right), \text{ if } c_{\mathrm{in}}^+ > c_{\mathrm{in,CR}}^+ \text{ or } (l_{\mathrm{l}} < L) \end{cases} \tag{7}$$

Where k_{D1}^+ is the dimensionless droplet deposition coefficient on the dry region of the test section, p is the sticking efficiency of droplets on the liquid film, $c_{\mathrm{in}}^+ = c_{\mathrm{in}}/\rho_{\mathrm{G}}$ is the dimensionless droplet concentration at the inlet of the test section, μ_{L} and μ_{G} are the viscosity of the liquid and the gas, respectively, $\mathrm{Re_{LFC}} = 4M_{\mathrm{LFC}}/D\pi\mu_{\mathrm{L}}$ is the critical Reynolds number of the liquid film (minimum value of $\mathrm{Re_{LF}}$ at which a steady liquid film exists) and $\mathrm{Re_G} = 4M_{\mathrm{G}}/D\pi\mu_{\mathrm{G}}$ is the Reynolds number of the gas.

4. Deposition data

The average dimensionless deposition coefficient k_{D}^+ is shown in Figs. 3 to 5. in terms of the dimensionless droplet concentration $c_{\mathrm{in}}^+ = c_{\mathrm{in}}/\rho_{\mathrm{G}}$ at the inlet of test section, are show in. Using Eq. (7) to fit the experimental data (c, k_{D1}^+) the values of the parameters k_{D1}^+, p, and $\mathrm{Re_{LFC}}$ are found and presented in Table 1. The values for k_{D1}^+ were found in the range 0.354 to 0.36, the values of p are in the range 0.305 to 0.325 and the $\mathrm{Re_{LFC}}$ are in the range from 0.425 to 2.9.

Equation (7) fits experimental data very well, as shown in Figs. 3 to 5. The RMS deviation of the fitting curve from the experimental data is in the range of the experimental accuracy of ±12%. The value of k_D^+ decreases as the droplet concentration at the test section inlet increases. An increase of the gas Reynolds number increases $\mathrm{Re_{LFC}}$.

As already mentioned, droplet impacting at small angles rebound from wetted surfaces, while there was no rebound from dry rough surfaces [26,27,28]. Relating the droplet deposition coefficient to the droplet concentration correlates the data very well. More experimental data from similar measurements are needed to precisely determine the three important parameters: the droplet deposition coefficient for the dry surface, the droplet sticking efficiency and the critical Reynolds number for a continuous wall liquid film. The critical Reynolds number depends on the fluid properties, the flow rates of fluids and the properties of the surface, in particular its wettability and roughness.

Table 1. Calculated parameters from the fitting by Eq. (7).

$\mathrm{Re_G}$	d_{10}, μm	τ^+	k_{D1}^+	p	$\mathrm{Re_{LFC}}$
40300	16.5	302	0.354	0.305	0.425
44700	16.2	296	0.354	0.31	0.54
67800	16.1	284	0.360	0.31	1.60
83500	8.2	237	0.360	0.32	2.40
93000	7.1	224	0.360	0.325	2.90

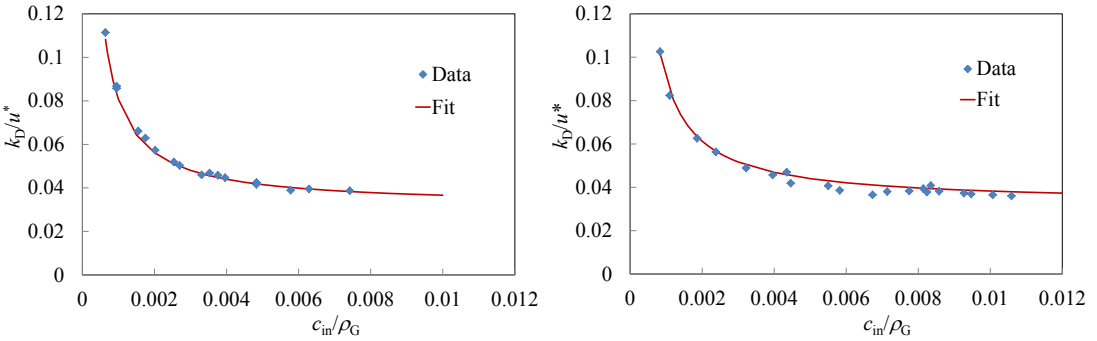

Fig. 3. Deposition coefficient at Re_G=40300, τ^+=302 (left) and at Re_G=44700, τ^+=296 (right).

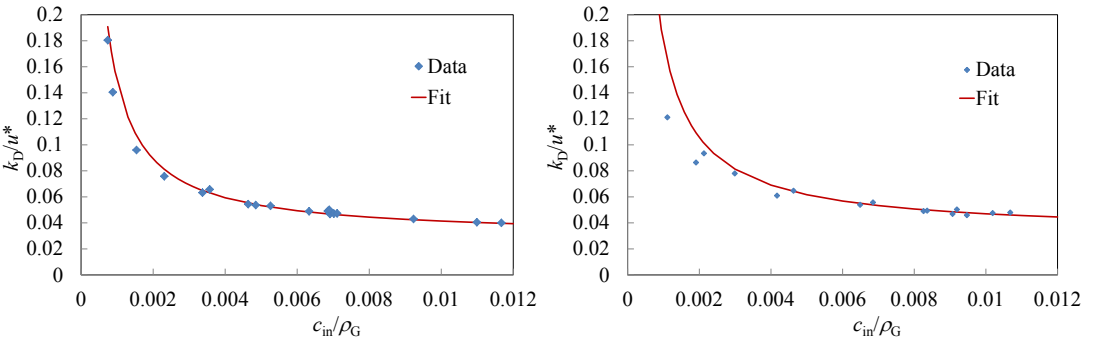

Fig. 4. Deposition coefficient at Re_G=47800, τ^+=284 (left) and at Re_G=83500, τ^+=237 (right).

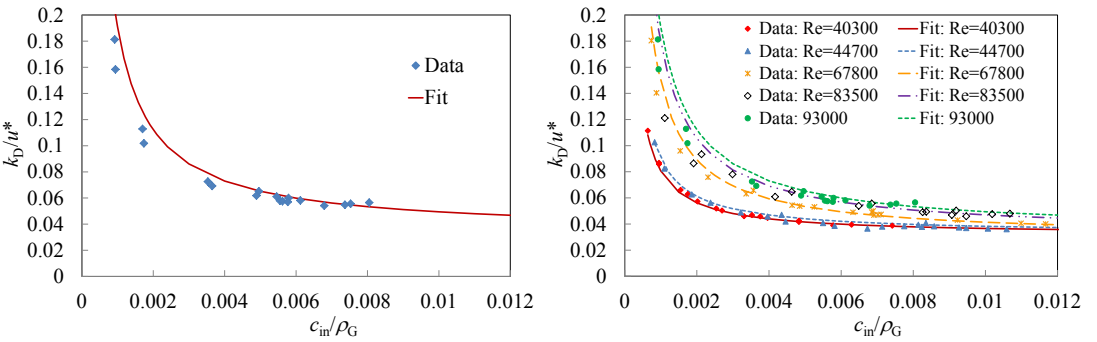

Fig. 5. Deposition coefficient at Re_G=93000, τ^+=224 (left) and comparison of deposition coefficients at Re_G from 43700 to 93000 (right).

Conclusion

This study is a part of an ongoing research effort which aims to improve our understanding of the vertical dispersed flow modelling. Presented data are based on the average droplet deposition coefficient in the test section. The droplets in annular dispersed flows approach to the tube wall at very low angles. The droplets rebound, thus leading to a significant decrease in the rate of deposition [28].

Eq. (7) successfully fits the given data sets and regression analysis enables us to estimate the key parameters of Eq. 7, i.e. k_{D1}^{+} ranging from 0.354 to 0.36, p which ranges from 0.305 to 0.325, and $\mathrm{Re}_{\mathrm{LFC}}$ which ranges from 0.425 to 2.9 depending on the gas Reynolds number. The dimensionless deposition coefficients for dry surfaces calculated from these experimental data are two times larger than those obtained for the fully annular flow.

A comparison of experimental results of this study with the available data on the deposition in annular flows is questionable. There are differences between the experiment reported in this paper, where the droplets are formed by an atomizer, and the experiments with a fully developed annular flow where the droplets are generated by entrainment from the wall liquid film. In a fully developed annular flow there are no "dry" regions, and it is not possible to measure or to predict the droplet sticking efficiency, because the wavy liquid film in an annular flow affects the droplet deposition. The gas flow creates waves and leads to a high deposition flux and high sticking efficiency.

The droplet deposition on a dry heated surface is a common process in post dryout regimes and the data estimated from the present experimental investigation can be used for a more accurate modelling of the droplet evaporation upon the impact on the heated wall.

This investigation provides experimental data that extend the knowledge about the droplet deposition and improve the models that involve the droplet sticking efficiency. The data allow further insight into the droplet deposition mechanisms that are important in modelling of the heat transfer in dispersed flows where the dispersed stream is in a direct contact with the wall, as in the post dry-out regimes, in modelling of spray coating and painting, and in surface cooling and liquid spreading.

The presence of a liquid film over the surface alters the boundary conditions, as the impact event in such case involves liquid–liquid interactions, though surface characteristics may still be important, depending on the surface roughness and the film thickness. Therefore, the future experiment will use test sections made of different materials (e.g. Plexiglas, PVC, copper) to investigate the influence of wettability and roughness on the droplet deposition coefficient.

Acknowledgements

The authors would like to thank the Department for Fluid Mechanics and Aerodynamics (SLA) at the Technical University of Darmstadt, for providing the research facilities required to conduct this research and the German Academic Exchange Service (DAAD) for its support through the research scholarship.

References

[1] L.B. Cousins, G.F. Hewitt, Liquid phase mass transfer in annular two-phase flow: droplet deposition and liquid entrainment, AERE-R5657 (1968).
[2] P.G. Papavergos, A.B. Hedley, Particle deposition behaviour from turbulent flows, Chem. Eng. Res. Des. 62 (1984) 275-295.
[3] A. Guha, Transport and deposition of particles in turbulent and laminar flow, Annu. Rev Fluid Mech. 40 (2008) 311-341.
[4] R.A. Farmer, P. Griffit, W.M. Rohsenow, Liquid droplet deposition in two-phase flow, J. Heat Transfer 92 (1970) 587-594
[5] L.F. Forney, L.A. Spielman, L.A, Deposition of coarse aerosols from turbulent flow, J. Aerosol Sci. 5 (1974) 257-271.
[6] B.Y.H Liu, J.K. Agarwal, Experimental observations of aerosol deposition in turbulent flow, J. Aerosol Sci. 5 (1974) 145-155.
[7] M.M. Lee, T.J. Hanratty, The inhibition of droplet deposition by the presence of a liquid wall film, Int. J. Multiphase Flow 14 (1988) 129-140.
[8] E.N. Ganić, K. Mastanaiah, K. Investigation of droplet deposition from a turbulent gas stream. Int. J. Multiphase Flow 7 (1981) 401-422.
[9] A.H. Govan, G.F. Hewitt, D.G. Owen, G. Burnett, Wall shear stress measurements in vertical air–water annular two-phase flow, Int. J. Multiphase Flow 15 (1989) 307-325
[10] D.M. Jepson, B.J. Azzopardi, P.B. Whalley, The effect of gas properties on drops in annular flow, Int. J. Multiphase Flow 15 (1989) 327-339.
[11] S.A. Schadel, G.W. Leman, J.L. Binder, T.J. Hanratty, Rates of atomization and deposition in vertical annular flow, Int J. Multiphase Flow 16 (1990) 363-374.
[12] Š. Šikalo, Experimental investigation of droplet deposition in turbulent dispersed flow, MSc. Thesis, University of Sarajevo, 1992.
[13] Š. Šikalo, N. Delalić, E.N. Ganić, Hydrodynamics and heat transfer investigation of air–water dispersed flow, Exp. Therm. Fluid Sci. 25 (2002) 511-521.
[14] S. Namie, T. Ueda, Droplet transfer in two-phase annular mist flow: II. Prediction of droplet transfer rate, Bull. J.S.M.E. 16 (1973) 752-764.
[15] J.W. Cleaver, B. Yates, A sub layer model for the deposition of particles from a turbulent flow, Chem. Eng Sci. 30 (1975) 983-992.
[16] J.L. Binder, T.J. Hanratty, A diffusion model for droplet deposition in gas/liquid annular flow, Int. J. Multiphase Flow 17 (1991) 1-11.
[17] J. Young, A. Leeming, A theory of particle deposition in turbulent pipe flow, J. Fluid Mech, 340 (1997) 129-159.

[18] P. Andreussi, Droplet transfer in two-phase annular flow, Int. J. Multiphase Flow 9 (1983) 697-713.
[19] G.F. Hewitt, A.H. Govan, Phenomenological modelling of non-equilibrium flows with phase change. Int. J. Heat. Mass Transfer 33 (1990) 229-242.
[20] K.J. Hay, Z.C. Liu, T.J. Hanratty, Relation of deposition to drop size when the rate law is nonlinear. Int. J. Multiphase Flow 22 (1996) 829-848.
[21] A. Soldati, P. Andreussi, The influence of coalescence on droplet transfer in vertical annular flow, Chem Eng Sci. 51 (1996) 353-363.
[22] T. Okawa, A. Kotani, I. Kataoka, Experiments for liquid phase mass transfer rate in annular regime for a small vertical tube, Int. J. Heat Mass Transfer 48 (2005) 585-598.
[23] T. J. Hanratty, Physics of Gas–Liquid Flows, Cambridge University Press, New York (2013).
[24] G. Cossali, A. Coghe, M. Marengo, The impact of a single drop on a wetted solid surface, Exp. Fluids 22 (1997) 463-472.
[25] K. Pan, C. Law, Dynamics of droplet-film collision, J. Fluid Mech., 587 (2007) 1-22.
[26] Š. Šikalo, Analysis of droplet impact onto horizontal and inclined surfaces, Dissertation, Technical University of Darmstadt (2002).
[27] Š. Šikalo, I. Bijelonja, Experimental and numerical simulation of droplet deposition on solid surfaces. Annals of DAAAM for 2003 & Proceedings of the 14th International DAAAM Symposium (2003) 413-414.
[28] Š. Šikalo, C. Tropea, E.N. Ganić, Impact of droplet onto inclined surfaces, J. Colloid Interf Sci. 286 (2005) 661-669.
[29] Š. Šikalo, E.N. Ganić, Phenomena of droplet–surface interactions, Exp. Therm. Fluid Sci. 31 (2006) 97-110.
[30] E. Berberović, N.P. van Hinsberg, S. Jakirlić, I.V. Roisman, C. Tropea, Drop impact onto a liquid layer of finite thickness: Dynamics of the cavity evolution, Phys. Rev. E 79 (2009) 036306.
[31] I.V. Roisman, E. Berberović, C. Tropea, Inertia dominated drop collisions. I. On the universal flow in the lamella, Phys. Fluids 21 (2009) 052103.
[32] E. Berberović, I.V. Roisman, S. Jakirlić, C. Tropea, Inertia dominated flow and heat transfer in liquid drop spreading on a hot substrate, Int. J. Heat Fluid Flow 32 (2011) 785-795.
[33] M.J. Meholic, D.L. Aumiller Jr., F.B. Cheung, A Mechanistic Model for Droplet Deposition Heat Transfer in Dispersed Flow Film Boiling, Nucl. Technol. 181 (2013) 106-114.
[34] A. Al-Sarkhia, C. Saricab, B. Qureshia, Modeling of droplet entrainment in co-current annular two-phase flow: A new approach, Int. J. Multiphase Flow 39 (2012) 21-28.
[35] X. Gao, R. Li, Spread and recoiling of liquid droplets impacting solid surfaces, AIChE J. 60 (2014) 2683-2691.
[36] Q. Li, Z. Chai, B. Shi, H. Liang, Deformation and breakup of a liquid droplet past a solid circular cylinder: A lattice Boltzmann study, Phys. Rev. E 90 (2014) 043015
[37] N. Laan, K.G. de Bruin, D. Bartolo, C. Josserand, D. Bonn, Maximum Diameter of Impacting Liquid Droplets, Phys. Rev. Appl 2 (2014) 044018.
[38] D.F. Tatterson, J.C. Dallman, T.J. Hanratty, Drop size in annular gas–liquid flows, AIChE J. 23 (1997) 68-76.
[39] S. Nukiyama, Y. Tanasawa, An experiment on the atomization of liquid by means of an air stream, Report 4, T JSME 4 (1938) 86-93.